

# Stability of Three-Wheeled Vehicles with and without Control System

M. A. Saeedi<sup>1,\*</sup>, R. Kazemi<sup>2</sup>

<sup>1</sup> Ph.D student, <sup>2</sup> Associate professor, Department of Mechanical Engineering, K. N. Toosi University of Technology, Tehran, Iran.

\*m\_aminsaeidi@yahoo.com

## Abstract

In this study, stability control of a three-wheeled vehicle with two wheels on the front axle, a three-wheeled vehicle with two wheels on the rear axle, and a standard four-wheeled vehicle are compared. For vehicle dynamics control systems, the direct yaw moment control is considered as a suitable way of controlling the lateral motion of a vehicle during a severe driving maneuver. In accordance to the present available technology, the performance of vehicle dynamics control actuation systems is based on the individual control of each wheel braking force known as the differential braking. Also, in order to design the vehicle dynamics control system the linear optimal control theory is used. Then, to investigate the effectiveness of the proposed linear optimal control system, computer simulations are carried out by using nonlinear twelve-degree-of-freedom models for three-wheeled cars and a fourteen-degree-of-freedom model for a four-wheeled car. Simulation results of lane change and J-turn maneuvers are shown with and without control system. It is shown that for lateral stability, the three wheeled vehicle with single front wheel is more stable than the four wheeled vehicle, which is in turn more stable than the three wheeled vehicle with single rear wheel. Considering turning radius which is a kinematic property shows that the front single three-wheeled car is more under steer than the other cars.

**Keywords:** stability, three-wheeled vehicles, differential braking, vehicle dynamics control systems.

## 1. Introduction

Nowadays, automobile companies are involved in the design of more efficient vehicles improving the energetic efficiency and making them smaller for the best use of the current roads and streets. The idea of smaller, energy-efficient vehicles for personal transportation seems to naturally introduce the three wheel platform. Opinions normally run either strongly against or strongly in favor of the three wheel layout. Advocates point to a mechanically simplified chassis, lower manufacturing costs, and superior handling characteristics. Opponents decry the three-wheeler's propensity to overturn. Both opinions have merit. Three-wheelers are lighter and less costly to manufacture. But when poorly designed or in the wrong application, a three wheel platform is the less forgiving layout. When correctly designed, however, a three wheel car can light new fires of enthusiasm under tired and routine driving experiences. And

today's tilting three-wheelers, vehicles that lean into turns like motorcycles, point the way to a new category of personal transportation products of much lower mass, far greater fuel economy, and superior cornering power. Today, auto manufacturers to design more efficient cars to improve energy and also to make them smaller in order to better use on streets and roads are modern. A three wheeled car, also known as a tri-car or tri-car, is an automobile having either one wheel in the front for steering and two at the rear for power, two in the front for steering and one in the rear for power, or any other combination of layouts [1,2].

Many efforts are being made in automotive industries to develop the vehicle dynamics control (VDC) system which improves the lateral vehicle response in critical cornering situations by distributing asymmetric brake forces to the wheels. Some of the systems have already been commercialized and are being installed in passenger vehicles. The VDC system has a good potential of

becoming one of the chassis control necessities due to its significant benefit at little extra cost when installed on top of the ABS/TCS system. A critical lateral motion of a vehicle refers to the situation when the tire-road contactness can no longer be sustained. In such situations, the body side slip angle grows and the sensitivity of the yaw moment with respect to the steer angle suddenly diminishes. An addition of the steer angle can no longer increase the yaw moment, which is however needed to restore the vehicle stability. The target of the VDC system is to make the vehicle's lateral motion behave as commanded by the driver's steering action. To achieve this, the controller generates the yaw moment to restore the stability by distributing asymmetric brake forces to the wheels. In vehicles without VDC, the yaw moment can be generated only by the driver's steering action. In vehicles with the VDC, however, when a critical situation is detected, the brake force becomes exclusively under the control of the VDC and a compensating yaw moment is generated [3].

For VDC systems, the yaw moment control is considered as way of controlling the lateral motion of a vehicle during a severe driving maneuver. One of the most effective methods for improving the handling performance and active safety of ground vehicles in non-linear regimes is direct yaw moment control (DYC) [4, 5].

In order to find a suitable control law for DYC, it is necessary to have a deep understanding of vehicle dynamics and control system limitations. From the viewpoint of vehicle dynamics and tire characteristics, Furukawa and Abe [6] reviewed the several control methods proposed by previous researchers and emphasized that, as DYC is more effective on the vehicle motion control in a non-linear range of vehicle dynamics and tire characteristics, the reasonable control law should be take this nonlinearity in to consideration. Thus, they proposed the sliding control method for DYC and used it in their later works [7, 8].

Some researchers have emphasized only the development of the control logic of yaw moment control cooperated with 4WS ignoring how the yaw moment is generated [9, 10]. Other researchers proposed PID controls or LQ-optimal controls to compensate the error between the actual state and desired state of the vehicle [11,12,13]. Also, many studies have been done about controlling vehicle slip ratio to generate sufficient lateral forces and longitudinal forces [14]. However, most of them do not guarantee the robustness to uncertainty in vehicle parameters and disturbances that are intrinsically associated with vehicles.

Many methods have been studied and actively developed to improve a four-wheeled vehicle's lateral stability actively (Zanten et al., 1998; Nagai et al., 1999; Nagai et al., 2002; Shino et al., 2001; Shibahata et al., 1992, Song et al., 2007). However, there have only been a few studies on the lateral stability of a three-wheeled vehicle.

In the present study, comparing the stability control of three-wheeled vehicles and a four-wheeled one is the main goal which has never been done. In order to do this, a linear control system for direct yaw moment control, to improve the vehicle handling, is developed. The control law is developed by minimizing the difference between the predicted and the desired yaw rate responses. The method is based on individually controlling the braking force of each wheel. In the case of lateral stability, it will be shown that the three wheeled vehicle with two wheels on the rear axle is more stable. Moreover, comparing turning radii shows that the three-wheeled vehicle with a single front wheel is more under steer. The optimal control system is robust to changes, and also, has a suitable performance while imposing changes.

Simulation results indicate that when the proposed optimal controller is engaged with the models, satisfactory handling performances for three kinds of vehicles can be achieved.

This paper is organized as follows. First, two 12-degree-of-freedom dynamic models for three-wheeled cars and a 14-degree-of-freedom dynamic model for four-wheeled car are used. The main reason of adopting a 4-wheeled car in this paper is to verify the models of 3-wheeled cars and to compare the dynamic performance of three-wheeled cars with that of the 4-wheeled car. Then, tire dynamics is modeled. In order to improve the dynamic performance of vehicles, linear optimal control theory is used, and some design parameters for the control algorithm are presented. Next, the validation of the four-wheeled vehicle model, and the results of simulations in lane change and J-turn maneuvers are presented, and the effectiveness of the control system for three-wheeled cars are shown. Finally, Conclusions are provided.

## 2. Vehicle Modeling

In this research, the vehicle dynamic model is a nonlinear model with twelve degrees of freedom. This model is made up of a sprung mass and four unsprung masses. The vehicle body has six degrees of freedom which are translational motions in x, y, and z direction, and angular motions about those three axes. Roll, pitch, and yaw motions are the rotation about x, y, and z axes, respectively. Each of the wheels has translational motion in z direction and wheel spin

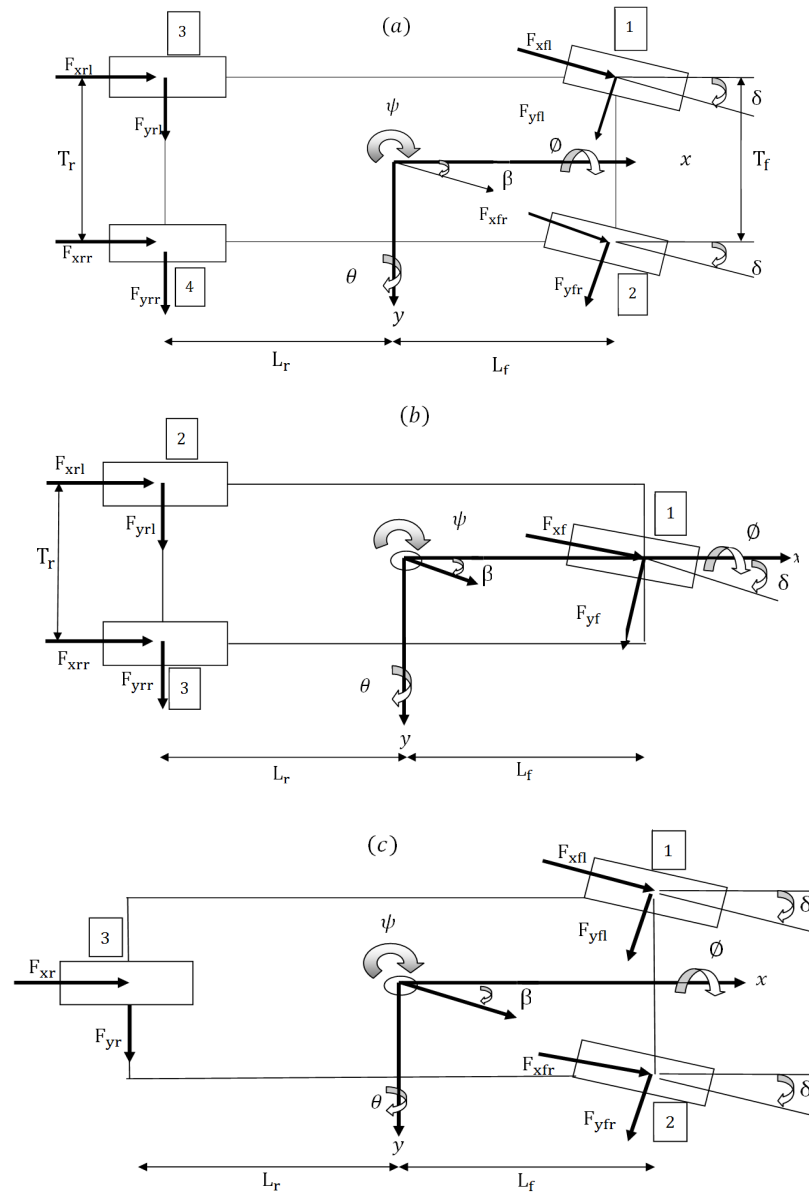


**Fig1.** (a) the fourteen-degree-of freedom model for four-wheeled vehicle, (b) the twelve-degree-of freedom model for three-wheeled car with front single wheel, (c) the twelve-degree-of freedom model for three-wheeled car with rear single wheel

about  $y$  direction. The front wheels can steer about the  $z$ -axis. It is worth noting that the four-wheeled vehicle model has fourteen degrees of freedom. The full vehicle models are shown in Fig.1. In the development of the vehicle model, the following assumptions were made:

1. The steering angles  $\delta$  of both front wheels are considered identical.
2. The effect of un sprung mass is ignored in the vehicle's pitch and roll motions.
3. The tire and suspension remain normal to the ground during vehicle maneuvers.

4. The center of roll and pitch motion are placed on the vehicle's center of gravity.

## 2.1 Equations of motion:

Governing equations of the Longitudinal, Lateral, and Vertical, Roll, Pitch and Yaw motions can be expressed as [5]:

**In Fig.1 (a):**

$$M_t(\dot{v}_x + \dot{\theta}v_z - v_y\dot{\psi}) = XF_{fl} + XF_{fr} + XF_{rl} + XF_{rr} \quad (1)$$

$$M_t(\dot{v}_y + v_x\dot{\psi} - \dot{\phi}v_z) = YF_{fl} + YF_{fr} + YF_{rl} + YF_{rr} \quad (2)$$

$$M_s(\dot{v}_z + \dot{\phi}v_y - \dot{\theta}v_x) = Fz_{fl} + Fz_{fr} + Fz_{rl} + Fz_{rr} \quad (3)$$

$$M_x = \sum \text{Roll Moments} = I_{sxx}\ddot{\phi} - (I_{syy} - I_{szz})\dot{\theta}\dot{\psi} = (Fz_{fr} - Fz_{fl})T_f/2 + (Fz_{rr} - Fz_{rl})T_r/2 - (YF_{fl} + YF_{fr} + YF_{rl} + YF_{rr})h \quad (4)$$

$$M_y = \sum \text{Pitch Moments} = I_{syy}\ddot{\theta} - (I_{szz} - I_{sxx})\dot{\theta}\dot{\psi} = (Fz_{rl} + Fz_{rr})l_r - (Fz_{fl} + Fz_{fr})l_f + (XF_{fl} + XF_{fr} + XF_{rl} + XF_{rr})h \quad (5)$$

$$M_z = \sum \text{Yaw Moments} = I_{zz}\ddot{\psi} - (I_{xx} - I_{yy})\dot{\phi}\dot{\theta} = (XF_{fl} - XF_{fr})T_f/2 + (XF_{rl} - XF_{rr})l_f + (YF_{fl} + YF_{fr})l_f - (YF_{rl} + YF_{rr})l_r + \sum_{i=1}^4 M_{zi} \quad (6)$$

Where  $\dot{\phi}$  is the roll rate, and  $\dot{\theta}$  is the pitch rate, and  $\dot{\psi}$  is the yaw rate. Also,  $M_{zi}$  is the tire self aligning torque. The terms  $XF_{ik}$  and  $YF_{ik}$  are the respective tire forces in the  $x$  and  $y$  directions, which can be related to the tractive and the lateral tire forces.

$$F_{ik} = Fx_{ik} \cos(\delta_{ik}) - Fy_{ik} \sin(\delta_{ik}) \text{ for } ((i = f, r), (k = l, r)) \quad (7)$$

$$YF_{ik} = Fy_{ik} \cos(\delta_{ik}) + Fx_{ik} \sin(\delta_{ik}) \text{ for } ((i = f, r), (k = l, r)) \quad (8)$$

#### Tire Side Slip Angle:

The angle between tire directions of motion has known as tire side slip angle and obtain based on the following formulation.

$$\alpha_1 = \tan^{-1} \left( \frac{v_y + l_f \dot{\psi}}{v_x + T_f/2 \dot{\psi}} \right) - (\delta_f) \quad (9)$$

The equations of motion for the suspension model are as follows:

$$\begin{aligned} Fz_{fl} &= ks_1(z_{u1} - z_1) + cs_1(\dot{z}_{u1} - \dot{z}_1) \\ Fz_{fr} &= ks_2(z_{u2} - z_2) + cs_2(\dot{z}_{u2} - \dot{z}_2) \\ Fz_{rl} &= ks_3(z_{u3} - z_3) + cs_3(\dot{z}_{u3} - \dot{z}_3) \\ Fz_{rr} &= ks_4(z_{u4} - z_4) + cs_4(\dot{z}_{u4} - \dot{z}_4) \end{aligned} \quad (10)$$

And

$$\begin{aligned} z_{fl} &= z_c - (T_f/2 \phi) - l_f \theta \\ z_{fr} &= z_c + (T_f/2 \phi) - l_f \theta \\ z_{rl} &= z_c - (T_r/2 \phi) + l_r \theta \\ z_{rr} &= z_c + (T_r/2 \phi) + l_r \theta \end{aligned} \quad (11)$$

In Fig.1 (b):

$$M_t(\dot{v}_x + \dot{\theta}v_z - v_y\dot{\psi}) = XF_f + XF_{rl} + XF_{rr} \quad (12)$$

$$M_t(\dot{v}_y + v_x\dot{\psi} - \dot{\phi}v_z) = YF_f + YF_{rl} + YF_{rr} \quad (13)$$

$$M_s(\dot{v}_z + \dot{\phi}v_y - \dot{\theta}v_x) = Fz_f + Fz_{rl} + Fz_{rr} \quad (14)$$

$$M_x = \sum \text{Roll Moments} = I_{sxx}\ddot{\phi} - (I_{syy} - I_{szz})\dot{\theta}\dot{\psi} = (Fz_{rr} - Fz_{rl}) \quad (15)$$

$$M_y = \sum \text{Pitch Moments} = I_{syy}\ddot{\theta} - (I_{szz} - I_{sxx})\dot{\theta}\dot{\psi} = (Fz_{rl} + Fz_{rr})l_r - (Fz_{fl} + Fz_{fr})l_f + (XF_f + XF_{rl} + XF_{rr})h \quad (16)$$

$$M_z = \sum \text{Yaw Moments} = I_{zz}\ddot{\psi} - (I_{xx} - I_{yy})\dot{\phi}\dot{\theta} = (XF_{rl} - XF_{rr})T_r/2 - (YF_{rl} + YF_{rr})l_r + (YF_f l_f) + \sum_{i=1}^3 M_{zi} \quad (17)$$

#### Tire Side Slip Angle:

$$\begin{aligned} \alpha_1 &= \tan^{-1} \left( \frac{v_y + l_f \dot{\psi}}{v_x} \right) - (\delta_f) \\ \alpha_2 &= \tan^{-1} \left( \frac{v_y - l_r \dot{\psi}}{v_x + T_r/2 \dot{\psi}} \right) \\ \alpha_3 &= \tan^{-1} \left( \frac{v_y - l_r \dot{\psi}}{v_x - T_r/2 \dot{\psi}} \right) \end{aligned} \quad (18)$$

In Fig.1 (c):

$$M_t(\dot{v}_x + \dot{\theta}v_z - v_y\dot{\psi}) = XF_{fl} + XF_{fr} + XF_r \quad (19)$$

$$M_t(\dot{v}_y + v_x\dot{\psi} - \dot{\phi}v_z) = YF_{fl} + YF_{fr} + YF_r \quad (20)$$

$$M_s(\dot{v}_z + \dot{\phi}v_y - \dot{\theta}v_x) = Fz_{fl} + Fz_{fr} + Fz_r \quad (21)$$

$$M_x = \sum \text{Roll Moments} = I_{sxx}\ddot{\phi} - (I_{syy} - I_{szz})\dot{\theta}\dot{\psi} = (Fz_{fr} - Fz_{fl})T_f/2 - (YF_{fl} + YF_{fr} + YF_r)h \quad (22)$$

$$\begin{aligned}
 M_y &= \sum \text{Pitch Moments} \\
 &= I_{syy} \ddot{\theta} - (I_{szz} - I_{sxx}) \dot{\theta} \dot{\psi} \\
 &= F_{zr} l_r - (F_{zf_l} + F_{zf_r}) l_f \\
 &\quad + (X F_{f_l} + X F_{f_r} + X F_r) h \quad (23)
 \end{aligned}$$

$$\begin{aligned}
 M_z &= \sum \text{Yaw Moments} = I_{zz} \ddot{\psi} - (I_{xx} - I_{yy}) \dot{\theta} \dot{\theta} \\
 &= (X F_{f_l} - X F_{f_r}) T_f / 2 + (Y F_{f_l} + Y F_{f_r}) l_f - (Y F_r l_r) \\
 &\quad + \sum_{i=1}^3 M_{zi} \quad (24)
 \end{aligned}$$

### Tire Side Slip Angle

$$\begin{aligned}
 \alpha_1 &= \tan^{-1} \left( \frac{v_y + l_f \dot{\psi}}{v_x + T_f / 2 \dot{\psi}} \right) - (\delta_f) \\
 \alpha_2 &= \tan^{-1} \left( \frac{v_y + l_f \dot{\psi}}{v_x - T_f / 2 \dot{\psi}} \right) - (\delta_f) \\
 \alpha_3 &= \tan^{-1} \left( \frac{v_y - l_r \dot{\psi}}{v_x} \right) \quad (25)
 \end{aligned}$$

### 2.2 Tire Dynamics

Apart from aerodynamic forces, all of the forces influencing the vehicle are created on the contact surface between the tire and the road. Hence, in the vehicle dynamic behavior simulation, the nonlinear

behavior of a tire is considered the most effective factor. In this model, the combined slip situation was modeled from a physical viewpoint. Tires generate lateral and longitudinal forces in a non-linear manner. In this paper, the combined slip Magic Formula of the tire model (1993) is used since it can provide considerable qualitative agreement between theory and the measured data. This model describes the effect of combined slip on the lateral force and on the longitudinal force characteristics. The general mathematical formulation of the Magic Formula model is presented in the Appendix, and reference [15].

### 2.3 Wheel Dynamics

The following equation can be written for traction, from Figure 2:

$$\dot{\omega}_i = \frac{1}{I_w} (T - r_w F_{xi}) \quad (26)$$

Note that in braking

$$\dot{\omega}_i = \frac{1}{I_w} (-T + r_w F_{xi}) \quad (27)$$

where  $\omega_i$  and  $F_{xi}$  denote rotational speed and longitudinal force associated with wheel  $i$ ,  $I_w$  is the spin inertia of the wheel,  $r_w$  is the tire rolling radius and  $T$  is the input drive or brake torque coming to the wheel [16].

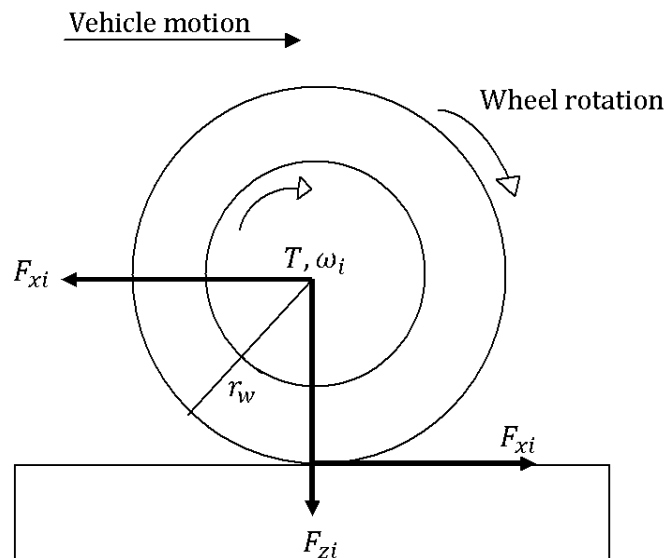


Fig2. wheel rotation [7]

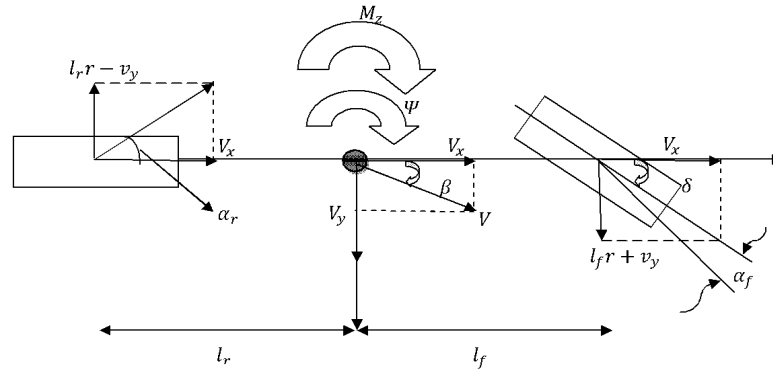


Fig3. Two-degree of freedom vehicle lateral dynamic model [18]

### 3. Controller Design

To improve the vehicle handling and stability, the yaw rate (the yaw velocity of the chassis) of the vehicle is controlled to follow its target value. For this purpose a linear control system is developed to control the three-wheeled car and also four-wheeled one. The control law consists of the disturbance feed-forward signal, which is related to the input steering angle, and the two state variable feedback terms being those of the yaw rate and the lateral velocity [17].

$$M_z = k_r r + k_v v + k_\delta \delta \quad (28)$$

$M_z$  Represents the control input and the front wheel steering angle  $\delta$  is considered as the external disturbance. A conventional linear two-degree of freedom model for vehicle handling, shown in Fig. 3, is developed. The governing equations for the yaw and lateral motions of the vehicle model are as follows [18]:

$$m \dot{v}_y + [mu + (2l_1 C_{\alpha_f} - 2l_2 C_{\alpha_r})/u]r + [(2C_{\alpha_f} + 2C_{\alpha_r})/u]v_y = 2C_{\alpha_f} \delta \quad (29)$$

$$I_{zz} \dot{r} + [(2C_{\alpha_f} l_1^2 + 2C_{\alpha_r} l_2^2)/u]r + [(2l_1 C_{\alpha_f} - 2l_2 C_{\alpha_r})/u]v_y = 2l_1 C_{\alpha_f} \delta + M_z \quad (30)$$

For the vehicle model, the lateral velocity  $v_y$  and the yaw rate  $r$  are considered as the two state

variables while the yaw moment  $M_z$  is the control input, which must be determined from the control law. Moreover, the vehicle steering angle  $\delta$  is considered as the external disturbance. In deriving the above equations, it is assumed that the steering angle is small and that the longitudinal force is ignored.

These equations in the state space form are shown as follows:

$$\dot{X} = AX + BM_z + E\delta \quad (31)$$

In Eq. (31),  $A$ ,  $B$ , and  $E$  are appropriate system matrices. The compensating yaw moment  $M_z$  is the control variable and the front wheel steer angle  $\delta$  is regarded as a disturbance. Where the matrices  $A$ ,  $B$  and  $E$  are defined as:

$$X = \begin{pmatrix} v_y \\ r \end{pmatrix} \quad A = \begin{pmatrix} a_{11} & a_{12} \\ a_{21} & a_{22} \end{pmatrix} \quad B = \begin{pmatrix} 0 \\ 1/I_{zz} \end{pmatrix} \quad E = \begin{pmatrix} 2C_{\alpha_f}/m \\ 2l_1 C_{\alpha_f}/I_{zz} \end{pmatrix}$$

$$a_{11} = -(2C_{\alpha_f} + 2C_{\alpha_r})/u \quad a_{12} = -u + (2l_2 C_{\alpha_r} - 2l_1 C_{\alpha_f})/mu$$

$$a_{21} = (2l_2 C_{\alpha_r} - 2l_1 C_{\alpha_f})/u \quad a_{22} = -(2C_{\alpha_f} l_1^2 + 2C_{\alpha_r} l_2^2)/u \quad (32)$$

#### 3.1 Desired Vehicle Performance

For vehicle dynamic control, the lateral velocity and yaw rate are selected as the control targets. The control system is designed to make the output of the actual vehicle follow the desired control target. The objective of the yaw rate controller is to minimize the error between the vehicle yaw rate and the desired yaw rate. In stationary turns, a definite relationship

exists between the steering angle, the vehicle longitudinal velocity, and the yaw rate. This relationship is used to drive the desired yaw rate [19]:

$$r_d = \frac{u}{l \left( 1 + \frac{k_{us}}{l} u^2 \right)} \delta \quad (33)$$

Where  $k_{us}$  is usually referred to as the under steer coefficient.

It is important to note that the control effort  $Mz$  must satisfy some physical constraints due to both the actuation system and the road-tire performance limits. To satisfy those limits, the control effort  $Mz$  in the performance index must be written as in the following form [17].

$$J = \frac{1}{2} \int_{t_0}^{t_f} [(r - r_d)^2 + wMz^2] dt \quad (34)$$

To determine the values of the feedback and feed-forward control gains, which are based on the defined performance index and the vehicle dynamic model, a LQR problem has been formulated for which its analytical solution is obtained, [20].

In that case, the performance index of Eq. (34) may be rewritten in the following form

$$J = \frac{1}{2} \int_0^\infty [(X_d - X)^T Q (X_d - X) + U^T R U] dt \quad (35)$$

Where

$$U = [Mz], \quad R = [w], \quad X_d = \begin{pmatrix} 0 \\ r_d \end{pmatrix} \quad (36)$$

The Hamiltonian function, in the expanded form, is given by:

$$H(u) = \frac{1}{2} U^T R U + \frac{1}{2} (X_d - X)^T Q (X_d - X) + P^T (AX + BU + E\delta) \quad (37)$$

Where  $X_d$  is the desired reference value of the state vector,  $Q$  is a real symmetric positive semi-definite matrix, and  $R$  is a real symmetric positive definite matrix, and

$$P = \begin{pmatrix} p_1 \\ p_2 \end{pmatrix} \quad (38)$$

Where the parameters  $p_1$  and  $p_2$  are the Lagrangian multipliers.

The costate equations are

$$\dot{P} = -\frac{\partial H}{\partial X} = Q(X_d - X) - A^T P \quad (39)$$

and the algebraic relations that must be satisfied are given by

$$\frac{\partial H}{\partial U} = RU + B^T P = 0 \quad (40)$$

$$\frac{\partial H}{\partial P} = AX + BU = \dot{X} \quad (41)$$

Therefore,

$$U = -R^{-1} B^T P \quad (42)$$

Considering that the current optimal control problem is a Tracking type, the matrix  $P$  is as following

$$P = KX + S \quad (43)$$

Next, by substituting eq. (43) into (42), we will have

$$U = -R^{-1} B^T (KX + S) \quad (44)$$

Differentiating both sides with respect to  $t$ , we obtain

$$\dot{P} = \dot{K}X + K\dot{X} + \dot{S} \quad (45)$$

Substituting from eq. (39) for  $\dot{P}$  and eq. (41) for  $\dot{X}$ , and using eq. (43) to eliminate  $P$ , the following relations can be obtained:

$$\dot{K} + A^T K + KA + Q - KBR^{-1}B^T K = 0 \quad (46)$$

$$\dot{S} + A^T S - KBR^{-1}B^T S - QX_d + E\delta = 0 \quad (47)$$

By assuming that the solutions of the equations converge rapidly to the constant values, therefore

$$\dot{K} = 0 \text{ and } \dot{S} = 0$$

Using the above assumptions, the following system of algebraic equations could then be formed:

$$A^T K + KA + Q - KBR^{-1}B^T K = 0 \quad (48)$$

$$(A^T + KBR^{-1}B^T)S - QX_d + E\delta = 0 \quad (49)$$

By solving equations (48) and (49) for  $K$  and  $S$ , the control input can be fully calculated.

#### 4. Simulation Results With The Vehicle Control System

##### Validation of Four-Wheel Vehicle Model

The actual test data and parameters of a passenger car are available [21]. Fig.6 (a, b) shows the comparison of the vehicle's lateral acceleration and yaw rate responses between the developed model and real test data during a constant-speed test. A ramp steering input was applied while the vehicle was running at a speed of 95 km/h. The test was carried out on a dry road. As shown, the responses of the vehicle model were well matched with the actual vehicle measurements. In order to verify the transient response of the developed model, the model is also validated with ADAMS/Car [22] in a J\_turn maneuvers at 50 km/h. Fig.6(c, d) shows the comparative yaw rate response. It can be seen that the developed model correlates very well with ADAMS/Car.

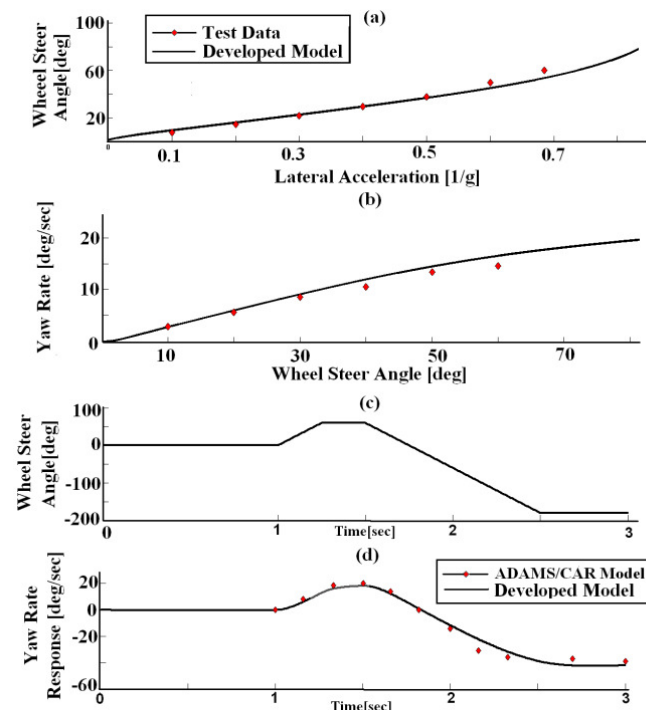


**Fig4.** Model validation results. with real test data: (a) Lateral acceleration. (b) Yaw rate response. With ADAMS/CAR: (c) Wheel steer angle. (d) Yaw rate response.

To study the transient performance of the proposed controller, numerical simulations are carried out with the aim of simulation software based on MATLAB and M-File for vehicles dynamic behavior during lane change and J-turn maneuvers between the cases with and without control. The effectiveness of the controller is shown considering two different steering angle inputs:

(a) a single lane change maneuver completed in 2s with two triangular pulses ( $\delta_f = \pm 3^\circ$ ).

(b) a J-turn maneuver produced from the ramp steer input ( $\delta_f = +3^\circ$ ).

It should be noted that all of the vehicle parameters are the same, and only in the cases of single wheel  $k_t$  and  $c_t$  coefficients are doubled.

#### 4.1 Vehicle dynamics under a single lane change maneuver

In this maneuver, the vehicles run on a level dry road with a friction coefficient of 0.7 at the constant speed of 110 km/h and the steering angle input shown in Fig.5 (a). In Figs.5 (b), (c) and (d) the

simulation results of vehicle dynamic characteristics are compared for three different vehicles.

Based on these results, three-wheeled vehicle with single rear wheel is highly unstable and deviates from the desired path. According to these tests, 3W1R car is stable only up to 80 km/h and shows a good dynamic performance, but, by increasing the longitudinal velocity it quickly becomes unstable. Three-wheeled vehicle with one front wheel is quite stable, and the desired yaw rate of the vehicle, that is the goal of stability in both maneuvers, is followed very well. Also, the desired yaw rate of the four-wheeled vehicle is not tracked well. After applying the desired control system, unstable 3W1R car becomes completely stable, and the desired yaw rate can be followed exactly. The 3W1F and 4W cars had relatively good stability before applying the controller. With the optimal control system the optimal path will be followed more. Results indicate that the controlled vehicles have better performances than the uncontrolled ones because the vehicle yaw rates trace their desired values.

#### 4.2 Vehicle Dynamics Under a J-turn Maneuver



Figure 6 shows the simulation results in a J-turn maneuver. The three-wheeled vehicle with rear single wheel is highly unstable, but the three-wheeled vehicle with one front wheel and four-wheeled vehicle are quite stable. The time response of yaw rates and the time response of side slip angles are shown in Fig.6 (b). Also, the results of the longitudinal velocity and lateral velocity together with lateral acceleration, vehicle trajectory for three vehicles are shown in Figs.6 (c) and (d). After applying the controller, performances of all of the three cars improve significantly, and they move in similar paths. It is obvious that the yaw moment control is able to improve dynamic performances of the vehicles and make them stable.

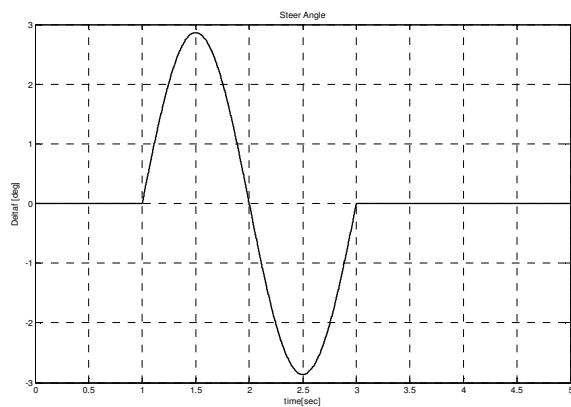
As it can be seen from Fig.6 (b), the side slips angle increases in the four-wheeled vehicle and the three-wheeled vehicle with single front wheel. It is obvious that in some cases using braking force on wheels in the control system results in more slipping in the lateral direction, and this causes the slip angle of the vehicle to increase. If this angle is in a suitable

range, there will not be an obstacle for vehicle motion. The main goal of this article is to control the yaw rate. For simultaneous control of  $r$  and  $\beta$ , more inputs are needed.

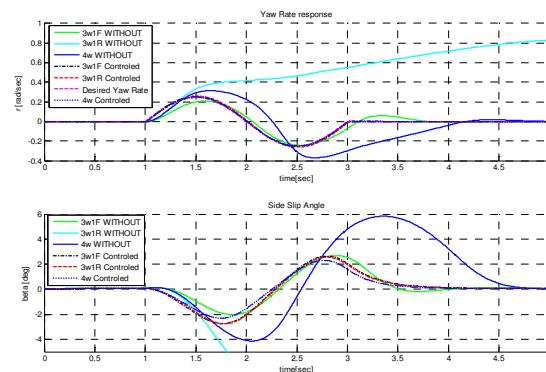
The role of  $\beta$  control is important under the condition that vehicle is in the unstable region, and controlling this variable results in a better control of the yaw rate. The velocities of the cars are increased slowly in order to make them have a path just like Fig.6 (e).

As it can be seen from Fig.6 (e), the turning radius of the 3W1F and 4W cars are larger than the turning radius of the 3W1R car. As a result, the 3W1F and 4W cars are understeer. The three-wheeled vehicle with rear single wheel due to having a rear wheel owns less cornering stiffness than the other vehicles.

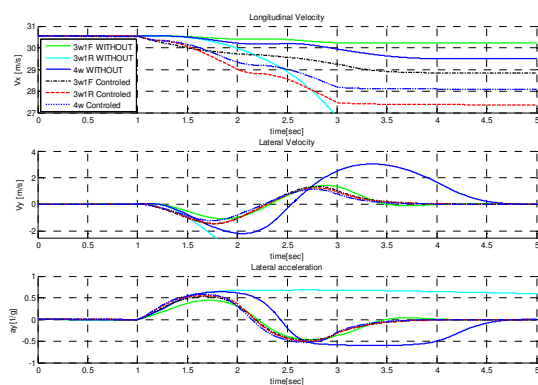
So, slip on the rear wheel increases, and as the vehicle is driven through the curve, the rear wheel loses adhesion before the front wheels causing the rear of the vehicle to slide outward.



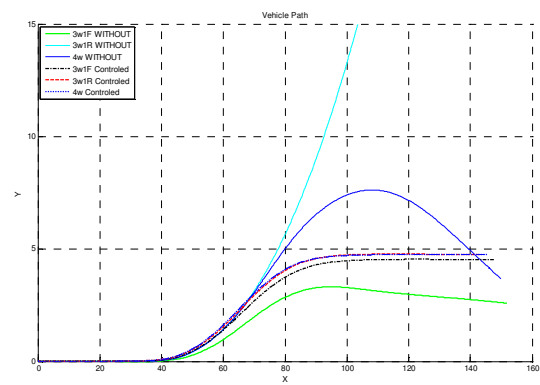
(a) steer angle



(b) yaw angular velocity and side slip angle



(c) longitudinal velocity, lateral velocity and lateral acceleration



(d) vehicle trajectory

Fig5. Simulation results of vehicles at lane change

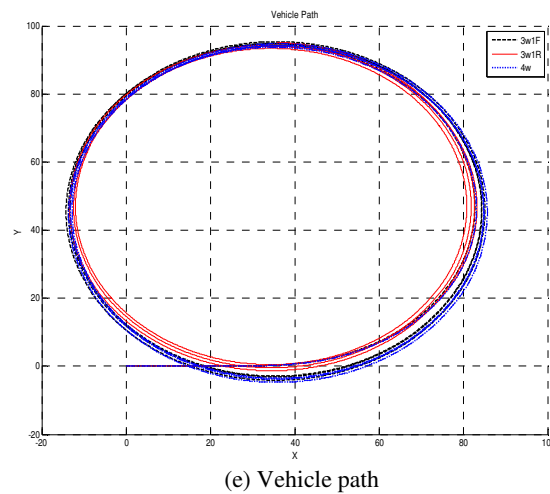


Fig6. Simulation results of vehicles at J-turn

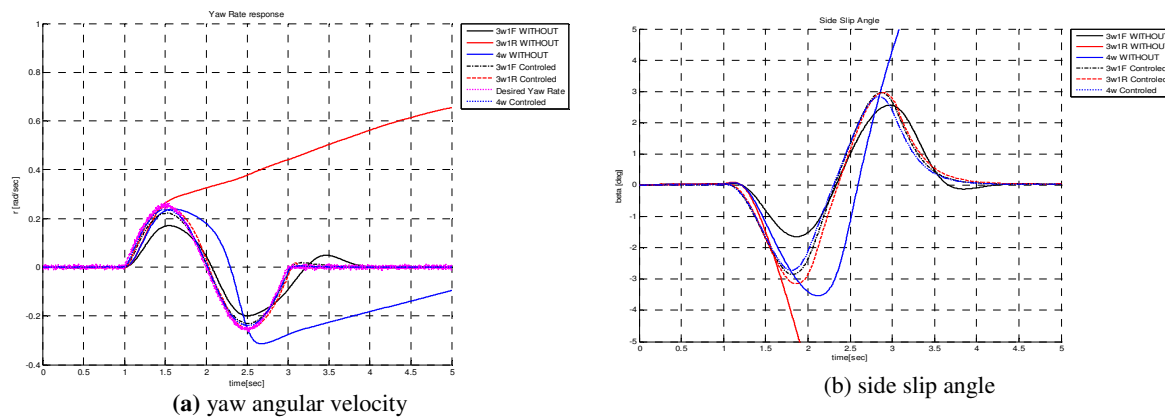


Fig7. Simulation results of vehicles at lane change.

As a result, the vehicle is pulled into the curve and becomes over steer, so the turning radius of the vehicle is smaller than that of a vehicle with neutral steer. Dynamic performance of the three-wheeled vehicle with one front wheel is much better than that of a four-wheeled vehicle. Therefore, the desired yaw rate is tracked better. The three-wheeled vehicle with one front wheel due to having a front wheel owns less cornering stiffness than the other vehicles. So, slip on the front wheel increases, and as the vehicle is driven through a curve, the front wheel loses adhesion before the rear wheels causing the front of the vehicle to be pulled outward the curve. As a result, it becomes under steer, and the turning radius of the vehicle increases correspondingly. To track the desired yaw rate, the controller generates the adequate yaw moment,  $M_z$ . The yaw moment is obtained from the control law and is converted into a braking torque in a way that if the yaw moment control is positive, the

braking torque is applied to the front and rear right wheels, and if it is negative, the braking torque is applied to the front and rear left wheels. These figures show that the response of the controlled system is better than that of the uncontrolled system.

In this section, the robust performance of the optimal controller under some changes like weight increase, closeness of the center of the gravity to the rear axle, and friction coefficient decrease is investigated.

Having made the changes, 3W1R and 4W cars become highly unstable, but the three-wheeled vehicle with front single wheel remains stable. After applying the controller, all the three cars become stable and follow the desired yaw rate. The variation of the optimal values of the feedback and feed forward gains with respect to the vehicle velocity is shown in Fig. 8.

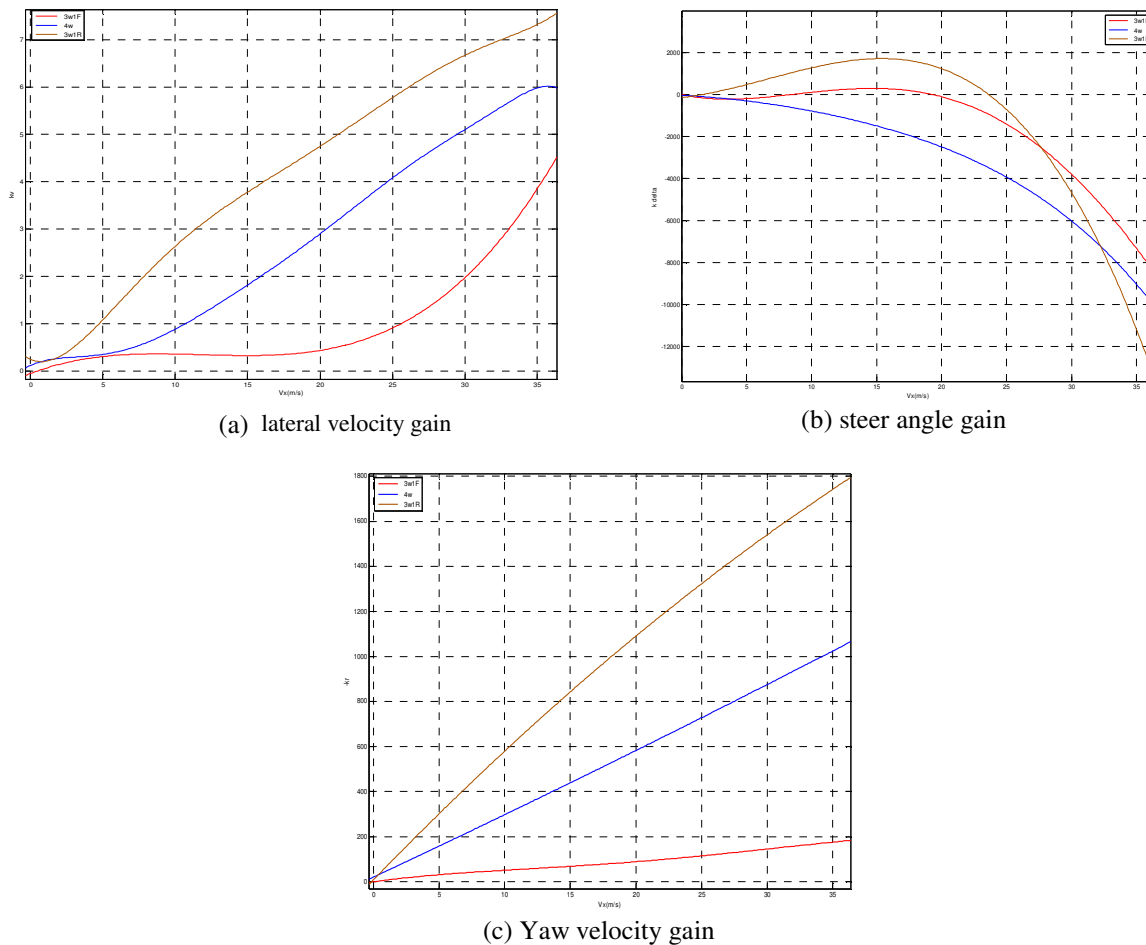


Fig8. variation of the optimal values of the feedback and feed-forward gains with the vehicle velocity

As it can be seen from Fig.8, the yaw velocity gain is always negative, and its magnitude increases rapidly when the vehicle longitudinal velocity increases. The lateral velocity gain has positive values, but its magnitude is relatively smaller than the yaw velocity gain. The variation of the steer angle gain with respect to the vehicle speed is completely different from those of the other two gains.

## 5. Conclusion

In this paper, dynamic performance and stability of three-wheeled cars were investigated.

Then, control system was designed based on the 2-degree-of-freedom model. Simulations results show that:

The three-wheeled vehicle with one front wheel without the controller has a better dynamic performance than four-wheeled vehicle in transient

conditions; therefore, the desired yaw rate is followed better in three-wheeled cars.

The three-wheeled vehicle with one rear wheel without the controller in higher speeds than 80 km/h is highly unstable, and it deviates from the desired path.

The controlled vehicles have a better performance in comparison with the uncontrolled vehicles because the control system can trace the desired response with a satisfactory accuracy.

in the case of lateral stability, the three wheeled vehicle with two wheels on the rear axle is more stable than the four wheeled vehicle, which is in turn more stable than the three wheeled vehicle with two wheels on the front axle.

The three-wheeled car with single front wheel is more under steer than the four-wheeled car, and the latter is more under steer than the three-wheeled car with single rear wheel.

The results obtained from this controller are quite general and can be used for other types of vehicles.

**Table 1.** Specification data for the vehicle under study.

Parameters	Content	Unit
$M_t$	1349	kg
$M_s$	1176	kg
$I_w$	1.1	kg.m <sup>2</sup>
$I_{xx}$	496	kg.m <sup>2</sup>
$I_{yy}$	2212	kg.m <sup>2</sup>
$I_{zz}$	2249	kg.m <sup>2</sup>
$L_f$	1.053	m
$L_r$	1.559	m
$h$	0.6053	m
$h_s$	0.5	m
$T_f$	1.483	m
$T_r$	1.483	m
$K_{sf}$	46800	N/m
$K_{sr}$	50000	N/m
$C_{sf}$	3000	N.s/m
$C_{sr}$	4000	N.s/m
$K_{tf}$	200000	N/m
$K_{tr}$	200000	N/m
$C_{tf}$	50	N.s/m
$C_{tr}$	50	N.s/m
$M_{uf}$	24.15	kg
$M_{ur}$	27.2	kg
$f_{roll}$	0.015	—
$Reff$	0.285	m

## REFERENCES

- [1]. Aga, M.; Okada, A. Analysis of vehicle stability control effectiveness from accident data, ESV Conference, Nagoya (2003).
- [2]. Farmer, Ch.: Effect of Electronic Stability Control on Automobile Crash Risk, IIHS Insurance Institute of Highway Safety, Arlington, Virginia, USA(2004).
- [3]. Park, K., Heo, S., Baek, I., Controller design for improving lateral vehicle dynamic stability, Society of Automotive Engineers of Japan, Vol.22, pp. 481–486(2001).
- [4]. Shibahata, Y., Shimada, K., and Tomari, T. Improvement of vehicle maneuverability by direct yaw moment control. Vehicle System Dynamics, Vol.22, 465–481(1993).
- [5]. Abe, M. Vehicle dynamics and control for improving handling and active safety: from four-wheel steering to direct yaw moment control. Proc. Instn. Mech. Engrs, Part K: J. Multi-body Dynamics, 213(K2), 87–101(1999).
- [6]. Furukawa, Y. and Abe, M. Advanced chassis control systems for vehicle handling and active safety. Vehicle System Dynamics, Vol.28, 59–86(1997).
- [7]. Mokhiamar, O. and Abe, M. Active wheel steering and yaw moment control combination to maximize stability as well as vehicle responsiveness during quick lane change for active vehicle handling safety. Proc. Instn. Mech. Engrs, Part D: J. Automobile Engineering, 216(D2), 115–124(2002).
- [8]. Mokhiamar, O. and Abe, M. How the four wheels should share forces in an optimum cooperative chassis control. Control Engng Practice, 14, 295–304(2006).
- [9]. M. Nagai, Y. Hirano, and S. Yamanaka, "Integrated control law of active rear wheel steering and direct yaw moment control," in Proc. of AVEC, pp. 451–469, (1996).
- [10]. M. Abe, N. Ohkubo, and Y. Kane, "A direct yaw moment control for improving limit performance of vehicle handling-comparison and cooperation with 4WS-" Vehicle System Dynamics, vol. 25, pp. 3–23, (1996).
- [11]. K. Koibuchi, M. Yamamoto, Y. Fukuda, and S. Inaga, "Vehicle stability control in limit cornering by active brake," SAE 960187, (1996).
- [12]. S. Matsumoto, H. Yamaguchi, H. Inoue, and Y. Yasuno, "Improvement of vehicle dynamics through braking force distribution control," SAE 920615, (1992).
- [13]. A. Alleyne, "A comparison of alternative intervention strategies for unintended roadway departure (URD) control," Proc. of AVEC, pp. 485–506, (1996).
- [14]. A. van Zanten, R. Erhardt, and G. Pfaff, "VDC, the vehicle dynamics control system of Bosch," SAE 950759, (1995).
- [15]. Pacejka, H.B., and Bakker, E. The combined slip Magic Formula tire model. In: Proceedings of 1st Colloquium on Tire Models for Vehicle Analysis, Delft 1991, ed. H.B. Pacejka, Suppl. Vehicle System Dynamics, 21, (1993).
- [16]. Kerem Bayar, Y. Samim Unlusoy. steering strategies for multi-axle vehicles, center for Automotive Research, the Ohio State University (2008).

- [17]. E. Esmailzadeh, A. Goodarzi, G.R. Vossoughi, "Optimal yaw moment control law for improved vehicle handling", Elsevier Science Ltd, (2001).
- [18]. Gillespie TD. Fundamentals of vehicle dynamics. Warrendale, PA, USA: Society of Automotive Engineers; (1992).
- [19]. Van Zanten, A. T., K. Erhardt, and G. Pfaff, "VDC, the vehicle dynamics control system of Bosch," SAE Paper, No. 950759 (1995).
- [20]. Kirk DE. Optimal control theory; an introduction. NewYork, NY, USA: Prentice-Hall; (1970).
- [21]. March, C. and Shim, T., "Integrated control of suspension and front steering to enhance vehicle handling," IMECHE, Part D: J. Automobile Engineering, Vol. 221, pp. 377-391, (2007).
- [22]. Shim, T. and C. Chike, "Understanding the limitations of different vehicle models for roll dynamics studies," Veh. Syst. Dyn., Vol. 45, No. 3, pp. 191–216 (2007).

## APPENDIX

### Notation

$M_t$	Vehicle total mass
$M_s$	Vehicle sprung mass
$I_w$	Wheel moment of inertia
$I_{xx}$	Roll moment of inertia
$I_{yy}$	Pitch moment of inertia
$I_{zz}$	Yaw moment of inertia
$L_f$	Distance of the center of gravity from the front axle
$L_r$	Distance of the center of gravity from the rear axle
$T_f$	Front track width
$T_r$	Rear track width
$M_{uf}$	Front unsprung mass
$M_{ur}$	Rear unsprung mass
$C_{si}$	Front/ rear suspension damping constant
$K_{si}$	Front/ rear suspension stiffness constant
$C_{ti}$	Front/rear tire damping constant
$K_{ti}$	Front/rear tire stiffness constant
$h_s$	Height of the sprung mass center of gravity
$f_{roll}$	Coefficient rolling resistance
$R_{eff}$	Effective wheel radiu